

THE ATACAMA COSMOLOGY TELESCOPE: A MEASUREMENT OF THE PRIMORDIAL POWER SPECTRUM

RENÉE HLOZEK¹, JOANNA DUNKLEY^{1,2,3}, GRAEME ADDISON¹, JOHN WILLIAM APPEL², J. RICHARD BOND⁴,
C. SOFIA CARVALHO⁵, SUDEEP DAS^{6,2,3}, MARK J. DEVLIN⁷, ROLANDO DÜNNER⁸, THOMAS ESSINGER-HILEMAN²,
JOSEPH W. FOWLER^{2,9}, PATRICIO GALLARDO⁸, AMIR HAJIAN^{4,3,2}, MARK HALPERN¹⁰, MATTHEW HASSELFIELD¹⁰,
MATT HILTON¹¹, ADAM D. HINCKS², JOHN P. HUGHES¹², KENT D. IRWIN⁹, JEFF KLEIN⁷, ARTHUR KOSOWSKY¹³,
TOBIAS A. MARRIAGE^{14,3}, DANICA MARSDEN⁷, FELIPE MENANTEAU¹², KAVILAN MOODLEY¹⁵, MICHAEL D. NIEMACK^{9,2},
MICHAEL R. NOLTA⁴, LYMAN A. PAGE², LUCAS PARKER², BRUCE PARTRIDGE¹⁶, FELIPE ROJAS⁸, NEELIMA SEHGAL¹⁷,
BLAKE SHERWIN², JON SIEVERS⁴, DAVID N. SPERGER³, SUZANNE T. STAGGS², DANIEL S. SWETZ^{7,9}, ERIC R. SWITZER^{18,2},
ROBERT THORNTON^{7,19}, ED WOLLACK²⁰

Draft version October 10, 2018

ABSTRACT

We present constraints on the primordial power spectrum of adiabatic fluctuations using data from the 2008 Southern Survey of the Atacama Cosmology Telescope (ACT). The angular resolution of ACT provides sensitivity to scales beyond $\ell = 1000$ for resolution of multiple peaks in the primordial temperature power spectrum, which enables us to probe the primordial power spectrum of adiabatic scalar perturbations with wavenumbers up to $k \simeq 0.2 \text{ Mpc}^{-1}$. We find no evidence for deviation from power-law fluctuations over two decades in scale. Matter fluctuations inferred from the primordial temperature power spectrum evolve over cosmic time and can be used to predict the matter power spectrum at late times; we illustrate the overlap of the matter power inferred from CMB measurements (which probe the power spectrum in the linear regime) with existing probes of galaxy clustering, cluster abundances and weak lensing constraints on the primordial power. This highlights the range of scales probed by current measurements of the matter power spectrum.

Subject headings:

1. INTRODUCTION

The cosmic microwave background (CMB) is light from the nascent universe, which probes early-universe physics. Measurements of the small-scale anisotropies of this radiation provide us with powerful constraints on many cosmological parameters, e.g., Reichardt et al. (2009); Sievers et al. (2009); Komatsu et al. (2010); Lueker et al. (2010); Dunkley et al. (2010).

In particular, the CMB constrains the power spectra of scalar and tensor perturbations, the relic observables associated with a period of inflation in the early universe (Wang et al. 1999; Tegmark & Zaldarriaga 2002; Bridle et al. 2003; Mukherjee & Wang 2003; Easther & Peiris 2006; Kinney et al. 2006; Bridges et al. 2007; Shafieloo & Souradeep 2007; Spergel et al. 2007; Verde & Peiris 2008; Reichardt et al. 2009; Chantavat et al. 2010; Bridges et al. 2009; Peiris & Verde 2010; Vazquez et al. 2011). The standard models of inflation predict a power spectrum of adiabatic scalar perturbations close to scale-invariant. Such models are often described in terms of a

¹ Department of Astrophysics, Oxford University, Oxford, UK
OX1 3RH

² Joseph Henry Laboratories of Physics, Jadwin Hall, Princeton University, Princeton, NJ, USA 08544

³ Department of Astrophysical Sciences, Peyton Hall, Princeton University, Princeton, NJ USA 08544

⁴ Canadian Institute for Theoretical Astrophysics, University of Toronto, Toronto, ON, Canada M5S 3H8

⁵ IPFN, IST, Av. Rovisco Pais, 1049-001 Lisboa, Portugal & RCAAM, Academy of Athens, Soranou Efessiou 4, 11-527 Athens, Greece

⁶ Berkeley Center for Cosmological Physics, LBL and Department of Physics, University of California, Berkeley, CA, USA 94720

⁷ Department of Physics and Astronomy, University of Pennsylvania, 209 South 33rd Street, Philadelphia, PA, USA 19104

⁸ Departamento de Astronomía y Astrofísica, Facultad de Física, Pontificia Universidad Católica de Chile, Casilla 306, Santiago 22, Chile

⁹ NIST Quantum Devices Group, 325 Broadway Mailcode 817.03, Boulder, CO, USA 80305

¹⁰ Department of Physics and Astronomy, University of British Columbia, Vancouver, BC, Canada V6T 1Z4

¹¹ School of Physics and Astronomy, University of Nottingham, University Park, Nottingham, NG7 2RD

¹² Department of Physics and Astronomy, Rutgers, The State University of New Jersey, Piscataway, NJ USA 08854-8019

¹³ Department of Physics and Astronomy, University of Pittsburgh, Pittsburgh, PA, USA 15260

¹⁴ Dept. of Physics and Astronomy, The Johns Hopkins University, 3400 N. Charles St., Baltimore, MD 21218-2686

¹⁵ Astrophysics and Cosmology Research Unit, School of Mathematical Sciences, University of KwaZulu-Natal, Durban, 4041, South Africa

¹⁶ Department of Physics and Astronomy, Haverford College, Haverford, PA, USA 19041

¹⁷ Kavli Institute for Particle Astrophysics and Cosmology, Stan-

ford University, Stanford, CA, USA 94305-4085

¹⁸ Kavli Institute for Cosmological Physics, Laboratory for Astrophysics and Space Research, 5620 South Ellis Ave., Chicago, IL, USA 60637

¹⁹ Department of Physics, West Chester University of Pennsylvania, West Chester, PA, USA 19383

²⁰ Code 553/665, NASA/Goddard Space Flight Center, Greenbelt, MD, USA 20771

spectral index n_s and an amplitude of perturbations $\Delta_{\mathcal{R}}^2$ as $\mathcal{P}(k) = \Delta_{\mathcal{R}}^2 \left(\frac{k}{k_0}\right)^{n_s-1}$, where k_0 is a pivot scale. A wide variety of models, however, predict features in the primordial spectrum of perturbations, which alter the fluctuations in the CMB (Amendola et al. 1995; Kates et al. 1995; Atrio-Barandela et al. 1997; Wang et al. 1999; Einasto et al. 1999; Kinney 2001; Adams et al. 2001; Matsumiya et al. 2002; Blanchard et al. 2003; Lasenby & Doran 2003; Hunt & Sarkar 2007; Barnaby & Huang 2009; Achúcarro et al. 2011; Nadathur & Sarkar 2010; Chantavat et al. 2010), which can be constrained using reconstruction of the primordial power.

Primordial fluctuations evolve over cosmic time to form the large scale structures that we see today. Therefore, a precision measurement of the power spectrum of these fluctuations, imprinted on the CMB, impacts all aspects of cosmology. Recent measurements of the CMB temperature and polarization spectra have put limits on the deviation from scale invariance including a variation in power-law with scale (e.g., a running of the spectral index, Kosowsky & Turner (1995)); in particular data from the Atacama Cosmology Telescope (ACT) (Das et al. 2010; Dunkley et al. 2010) combined with WMAP satellite data (Larson et al. 2010) find no evidence for running of the spectral index with scale and disfavor a scale-invariant spectrum with $n_s = 1$ at 3σ .

In this work we probe a possible deviation from power-law fluctuations by considering the general case where the power spectrum is parameterized as bandpowers within bins in wavenumber (or k) space. This ‘agnostic’ approach allows for a general form of the primordial power spectrum without imposing any specific model of inflation on the power spectrum, and facilitates direct comparison with a wide range of models. Such tests of the primordial power have been considered by various groups (Wang et al. 1999; Tegmark & Zaldarriaga 2002; Bridle et al. 2003; Hannestad 2003; Sealfon et al. 2005; Spergel et al. 2007; Verde & Peiris 2008; Peiris & Verde 2010; Vazquez et al. 2011). We revisit the calculation because of ACT high sensitivity over a broad range in angular scale.

This paper is based on data from 296 square degrees of the ACT 2008 survey in the southern sky, at a central frequency of 148 GHz. The resulting maps have an angular resolution of $1.4'$ and a noise level of between 25 and 40 μK per arcmin². A series of recent papers has described the analysis of the data and scientific results. The ACT experiment is described in Swetz et al. (2010), the beams and window functions are described in Hincks et al. (2009), while the calibration of the ACT data to WMAP is discussed in Hajian et al. (2010). The power spectra measured at 148 GHz and 218 GHz are presented in Das et al. (2010), and the constraints on cosmological parameters are given in Dunkley et al. (2010). A high-significance catalog of clusters detected through their Sunyaev-Zel’dovich (SZ) signature is presented in Marriage et al. (2010); the clusters are followed up with multi-wavelength observations described in Menanteau et al. (2010); the cosmological interpretation of these clusters is presented in Sehgal et al. (2011).

2. METHODOLOGY

2.1. Angular Power spectrum

Following the work of Wang et al. (1999); Tegmark & Zaldarriaga (2002); Bridle et al. (2003); Mukherjee & Wang (2003) and Spergel et al. (2007), we parameterize the primordial power spectrum $\mathcal{P}(k)$ using bandpowers in 20 bins, logarithmically spaced in mode k from $k_1 = 0.001$ to $k_{20} = 0.35 \text{ Mpc}^{-1}$, with $k_{i+1} = 1.36k_i$ for $1 < i < 19$. To ensure the power spectrum is smooth within bins, we perform a cubic spline such that:

$$\mathcal{P}(k) = \Delta_{\mathcal{R},0}^2 \times \begin{cases} 1 & \text{for } k < k_1 \\ A_i P_i + B_i P_{i+1} + \\ ((A_i^3 - A_i)C_i + (B_i^3 - B_i)C_{i+1}) \frac{h_i^2}{6} & \text{for } k_i < k < k_{i+1} \\ P_{20} & \text{for } k > k_{20} \end{cases} \quad (1)$$

where the P_i are the power spectrum amplitudes within bin i , normalised so that $P_i = 1$ corresponds to scale invariance. The $\Delta_{\mathcal{R},0}^2$ is a normalized amplitude of scalar density fluctuations, which we take to be 2.36×10^{-9} (Larson et al. 2010), and is the amplitude for a power-law spectrum around a pivot scale of $k_0 = 0.002 \text{ Mpc}^{-1}$. We do not vary the amplitude in our analysis as the power in the individual bands is degenerate with the overall amplitude; if a higher value was used, the estimated bandpowers would be lower by the corresponding amount, as we are measuring the total primordial power within a bin. The coefficients C_i are the second derivatives of the input binned power spectrum data (Press et al. 1992), $h_i = k_{i+1} - k_i$ is the width of the step and $A_i = (k_{i+1} - k)/h_i$ and $B_i = (k - k_i)/h_i$. We do not impose a ‘smoothness penalty’ as discussed in Verde & Peiris (2008) and in Peiris & Verde (2010). Adding more parameters to the parameter set makes it easier for the model to fit bumps and wiggles in the spectrum, hence as the number of bins increases, this parameterization will fit the noise in the data, particularly on large scales (small values of k). This in turn is expected to increase the goodness-of-fit of the model by approximately one per additional parameter. Hence, a model that fits the data significantly better than the standard ΛCDM power-law would yield an increase in the likelihood of more than one per additional parameter in the model. The logarithmic spacing in k means that this is less of a problem at high multipoles, as many measurements are used to estimate the power in each band.

The primordial power spectrum is related to the CMB power spectra through the radiation transfer functions $T_T(k)$, $T_E(k)$ and $T_B(k)$ (defined as in Komatsu & Spergel (2001)) as:

$$C_\ell^{\alpha\beta} \propto \int k^2 dk \mathcal{P}(k) T_\alpha(k) T_\beta(k) \quad (2)$$

where α and β index T, E or B , corresponding to temperature or the two modes of polarization. The correspondence between multipole ℓ and mode k (in Mpc^{-1})

is roughly $\ell \simeq kd$, where $d \simeq 14000$ Mpc is the comoving distance to the last scattering surface. Figure 1 shows schematically how the primordial power spectrum translates to the temperature angular power spectrum. In each case, a single step function is used for the primordial power spectrum in Eq. (2).

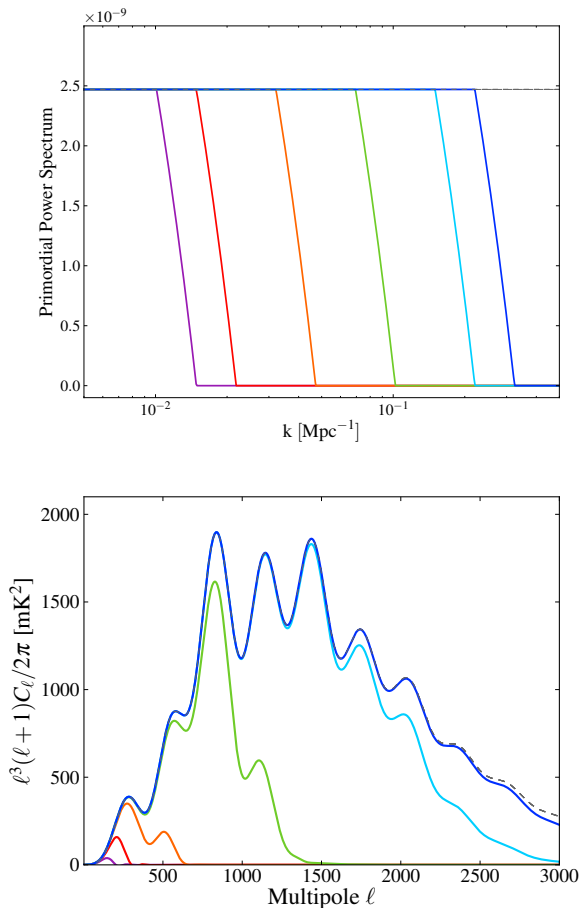


FIG. 1.— Stepping up in power: we show schematically the angular power spectrum (lower panel) resulting from building up the primordial power spectrum $\mathcal{P}(k)$ in bins (top panel), from $k = 0.007$ Mpc^{-1} (left-most curve in the top panel) to $k = 0.22$ Mpc^{-1} (right-most curve). The power in each case is normalized to a single amplitude before the step function, and set to zero afterwards, so that as more bins are added to the primordial spectrum, it tends towards a scale-invariant spectrum (shown as the dashed line). Correspondingly, the C_ℓ spectrum (plotted as $\ell^3(\ell+1)C_\ell^{TT}/2\pi$ mK^2 in the bottom panel) also tends to a spectrum characterized by $n_s = 1$, also shown as the grey dashed curve.

Previous analyses have only constrained the primordial power out to $k \lesssim 0.15$ Mpc^{-1} (Bridle et al. 2003; Spergel et al. 2007; Peiris & Verde 2010). The arcminute resolution of ACT means that one can constrain the primordial power out to larger values of k ($\simeq 0.19$ Mpc^{-1}). The primary CMB power spectrum decreases exponentially due to Silk damping (Silk 1968) at multipoles greater than $\ell \simeq 2000$, while the power spectrum from diffuse emission of secondary sources begins to rise from $\ell \simeq 2000$. The ACT measurement window between $1000 < \ell < 3000$ provides a new window with which to constrain any deviation from a standard power-law spectrum, as this is in the range of scales before the power from secondary

sources dominates. We use the 148 GHz measurements from the 2008 ACT Southern Survey, and include polarization and temperature measurements from the WMAP satellite with a relative normalization determined by Hajian et al. (2010). We use the ACT likelihood described in Dunkley et al. (2010) and the WMAP likelihood found in Larson et al. (2010).

2.2. Parameter estimation

Our cosmological models are parameterized using:

$$\Omega_c h^2, \Omega_b h^2, \theta_A, \tau, \mathbf{P}, \quad (3)$$

where $\Omega_c h^2$ is the cold dark matter density; $\Omega_b h^2$ is the baryon density; h is the dimensionless Hubble parameter such that $H_0 = 100h$ $\text{kms}^{-1}\text{Mpc}^{-1}$; θ_A is the ratio of the sound horizon to the angular diameter distance at last scattering, and is a measure of the angular scale of the first acoustic peak in the CMB temperature fluctuations; τ is the optical depth at reionization, which we consider to be ‘instantaneous’ (equivalent to assuming a redshift range of $\Delta z = 0.5$ for CMB fluctuations) and $\mathbf{P} = \{P_i\}$, $i = 1, \dots, 20$, is the vector of bandpowers where $P_i = 1 \forall i$ describes a scale-invariant power spectrum. We assume a flat universe in this analysis. In addition, we add three parameters, A_{SZ} , A_p , A_c , to model the secondary emission from the Sunyaev-Zel’dovich effect from clusters, Poisson-distributed and clustered point sources respectively, marginalizing over templates as described in Dunkley et al. (2010) and Fowler et al. (2010). We impose positivity priors on the amplitudes of these secondary parameters. We modify the standard Boltzmann code CAMB²¹ (Lewis & Challinor 2002) to include a general form for the primordial power spectrum, and generate lensed theoretical CMB spectra to $\ell = 4000$, above which we set the spectra to zero for computational efficiency, as the signal is less than 5% of the total power.

The likelihood space is sampled using Markov chain Monte Carlo methods. The probability distribution is smooth, single-moded and close to Gaussian in most of the parameters. These properties make the 27-dimensional likelihood space less demanding to explore than an arbitrary space of this size: the number of models in the Markov chain required for convergence scales approximately linearly with the number of dimensions. Sampling of the parameter space is performed using CosmoMC²² (Lewis & Bridle 2002). The analysis is performed on chains of length $N = 200000$. We sample the chains and test for convergence following the prescription in Dunkley et al. (2005), using an optimal covariance matrix determined from initial runs.

We impose limiting values on the power spectrum bands $0 < P_i < 10$ for all i . To avoid exploring regions of parameter space inconsistent with current astronomical measurements, we impose a Gaussian prior on the Hubble parameter today of $H_0 = 74.2 \pm 3.6$ from Riess et al. (2009).

²¹ <http://cosmologist.info/camb>

²² <http://cosmologist.info/cosmomc>

TABLE 1
ESTIMATED POWER SPECTRUM BANDS IN UNITS OF 10^{-9}

Wavenumber k (Mpc^{-1})	Power spectrum band ^{a,b}	WMAP only binned $\mathcal{P}(k)$	ACT+WMAP binned $P(k)$
0.0010	P_1	$4.99^{+1.79}_{-1.77}$	5.07 ± 1.82
0.0014	P_2	< 3.22	< 3.49
0.0019	P_3	< 3.04	< 3.03
0.0025	P_4	< 4.34	< 4.15
0.0034	P_5	3.32 ± 0.99	3.52 ± 1.05
0.0047	P_6	$2.31^{+0.60}_{-0.58}$	2.29 ± 0.64
0.0064	P_7	2.21 ± 0.33	2.27 ± 0.31
0.0087	P_8	2.43 ± 0.19	2.48 ± 0.20
0.0118	P_9	2.29 ± 0.15	2.35 ± 0.15
0.0160	P_{10}	2.31 ± 0.13	2.37 ± 0.12
0.0218	P_{11}	2.20 ± 0.11	2.28 ± 0.11
0.0297	P_{12}	2.38 ± 0.14	2.40 ± 0.13
0.0404	P_{13}	2.28 ± 0.23	2.39 ± 0.23
0.0550	P_{14}	1.98 ± 0.20	2.14 ± 0.14
0.0749	P_{15}	2.37 ± 0.53	$2.41^{+0.20}_{-0.28}$
0.1020	P_{16}	< 4.01	$2.20^{+0.71}_{-0.80}$
0.1388	P_{17}	—	$2.19^{+0.79}_{-0.87}$
0.1889	P_{18}	—	< 2.37
0.2571	P_{19}	—	< 2.40
0.3500	P_{20}	—	—

^a For one-tailed distributions, the upper 95% confidence limit is given, whereas the 68% limits are shown for two-tailed distributions.

^b The primordial power spectrum is normalized by a fixed overall amplitude $\Delta_{\mathcal{R},0}^2 = 2.36 \times 10^{-9}$ (Larson et al. 2010).

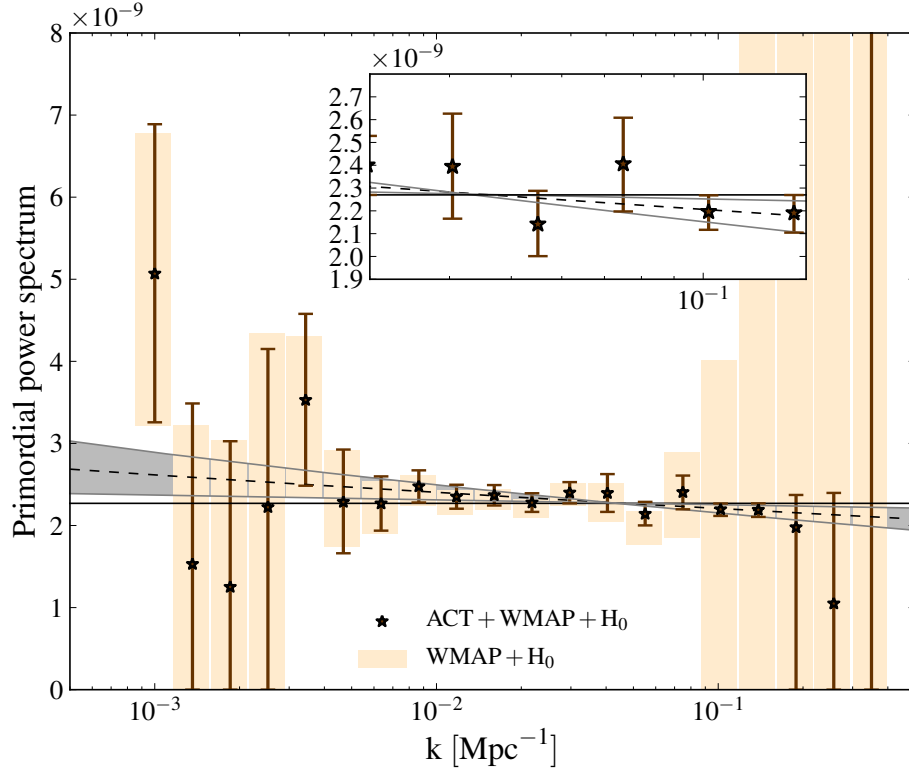


FIG. 2.— Primordial power constraints: the constraints on the primordial power spectrum from the ACT data in addition to WMAP data compared to the WMAP constraints alone. In both cases, a prior on the Hubble parameter from Riess et al. (2009) was included. Where the marginalised distributions are one-tailed, the upper errorbars show the 95% confidence upper limits. On large scales the power spectrum is constrained by the WMAP data, while at smaller scales the ACT data yield tight constraints up to $k = 0.19 \text{ Mpc}^{-1}$. The horizontal solid line shows a scale-invariant spectrum, while the dashed black line shows the best-fit ΛCDM power-law with $n_s = 0.963$ from Dunkley et al. (2010), with the spectra corresponding to the 2σ variation in spectral index indicated by solid band. The constraints are summarized in Table 1.

3. RESULTS

3.1. Primordial Power

Figure 2 shows the constraints on the primordial power spectrum from measurements of the cosmic microwave background. The shaded bands are the constraints on the power spectrum from WMAP measurements alone. Over this range of scales there is no indication of deviation from power-law fluctuations. As was shown in Spergel et al. (2007), the lack of data at multipole moments larger than $\ell = 1000$ restricts any constraints on the primordial power spectrum at $k > 0.1 \text{ Mpc}^{-1}$. In contrast, the combined ACT/WMAP constraints are significantly improved, particularly for the power at scales $0.1 < k < 0.19 \text{ Mpc}^{-1}$. The resulting power spectrum is still consistent with a power-law shape, with $n_s = 0.963$ (the best-fit value from Dunkley et al. (2010)). Despite the fact that we have added 18 extra degrees of freedom to the fit, a scale-invariant spectrum ($n_s = 1$, shown by the horizontal line on Fig. 2) is disfavored at 2σ . In addition, we find no evidence for a significant feature in the small-scale power. The bands at $k > 0.19 \text{ Mpc}^{-1}$ in the ACT+WMAP case are largely unconstrained by the data. Including 218 GHz ACT data will improve the measurements of the primordial power, since it will relieve the degeneracies between the binned primordial power, the clustered IR source power, and the Poisson source power, all of which provide power at $\ell > 2000$.

The estimated primordial power spectrum values are summarized in Table 1. The CMB angular power spectra corresponding to the allowed range in the primordial power spectrum (at 1σ) are shown in Figure 3 for WMAP-alone compared to WMAP and ACT combined. The temperature-polarization cross spectra corresponding to these allowed models are also shown in Figure 3, indicating how little freedom remains in the small-scale TE spectrum. This allowed range in C_ℓ^{TE} at multipoles $\ell > 1000$ will be probed by future CMB polarization experiments such as Planck (Planck Collaboration et al. 2011), ACTPol (Niemack et al. 2010) and SPTPol (Carlstrom et al. 2009).

In this analysis, we use a prior on the Hubble constant. Removing this prior reveals a degeneracy between the primordial power on scales $0.01 < k < 0.02 \text{ Mpc}^{-1}$ (bands P_{8-11} in Figure 4), and the set of parameters describing the contents and expansion rate of the universe. Both affect the first acoustic peak. This degeneracy was previously noted in, e.g., Blanchard et al. (2003); Hunt & Sarkar (2007); Nadathur & Sarkar (2010), where a power spectrum model “bump” at $k = 0.015 \text{ Mpc}^{-1}$ was found to be consistent with observations in the context of a low H_0 , and without any dark energy. Along this degeneracy, the primordial spectrum can be modified to move the position of the first peak to larger scales (relative to power-law), also increasing its relative amplitude. Since the first peak position is well measured by WMAP, this increase in angular scale is compensated by decreasing θ_A . In a flat universe, this corresponds to a decrease in the Hubble constant and the cosmological constant. The matter density increases to maintain the first peak amplitude. The baryon density then de-

creases to maintain the relative peak heights. Imposing a prior on the Hubble constant has the effect of breaking this degeneracy. Alternatively, one could impose a prior on the baryon density from Big Bang Nucleosynthesis ($\Omega_b h^2 = 0.022 \pm 0.002$) which would disfavor the low- H_0 models, as indicated in the top left panel of the bottom rows in Figure 4.

It is worth noting that the increase in the matter density along this degeneracy also increases the gravitational lensing deflection power, as a universe with a larger matter content exhibits stronger clustering at a given redshift. ACT maps have sufficient angular resolution to measure this deflection of the CMB (Das et al. 2011). Even without a strong prior on the Hubble constant, models with a bump in the primordial spectrum and $H_0 < 50$ (with $< 10\%$ Dark Energy density) are disfavored at $> 4\sigma$ from the lensing measurement alone, a result similar to that discussed in Sherwin et al. (2011). Although parameterized differently, the same argument applies to the primordial spectrum considered by Hunt & Sarkar (2007), motivated by phase transitions during inflation, that eliminates dark energy but which is also disfavored at $\simeq 3\sigma$ by the lensing for a standard cold dark matter model.

The estimated cosmological parameters are given in Table 2 and the marginalized one-dimensional likelihoods are shown in Figure 4. While the binned $P(k)$ model adds 18 additional parameters to the parameter set, only 13 of those parameters are well constrained. All cosmological parameters in the binned power spectrum model are consistent with those derived using the concordance 6-parameter model with a power-law primordial spectrum. The addition of 13 new parameters which are substantially constrained by the data increases the likelihood of the model such that $-2\ln\mathcal{L} = 9.3$. Using a simple model comparison criterion like the Akaike Information Criterion (e.g., Liddle 2004; Takeuchi 2000), the binned power spectrum model is disfavored over the standard concordance model. Further, we find a power-law slope fit to the 13 constrained bands in power spectrum space (bands labeled from P_5 to P_{17} in Figure 4) of $n_s = 0.965$, which is, as expected, consistent with the constraints on the spectral index from Dunkley et al. (2010).

3.2. Reconstructed $P(k)$

The primordial power spectrum translates to the angular power spectrum of the CMB, but can in addition be mapped to the late-time matter power spectrum through the growth of perturbations:

$$P(k, z=0) = 2\pi^2 k \mathcal{P}(k) G^2(z) T^2(k) \quad (4)$$

where $G(z)$ gives the growth of matter perturbations, $T(k)$ is the matter transfer function, and the $\mathcal{P}(k)$ are the fitted values as in Eq. (1). This mapping enables the constraints on the power spectrum from the CMB to be related to power spectrum constraints from other probes at $z \simeq 0$ (Tegmark & Zaldarriaga 2002; Bird et al. 2010). We illustrate the power spectrum constraints from the ACT and WMAP data in Figure 5. We take $G(z)$ and $T(k)$ from a Λ CDM model, but nei-

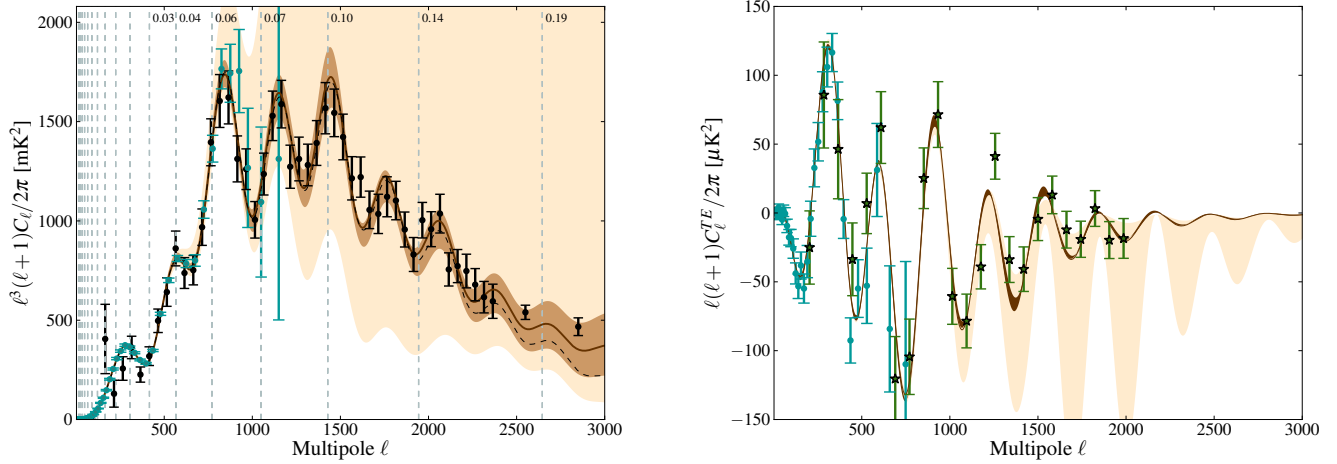


FIG. 3.— Mapping primordial power to the angular power spectrum: the constraints on the primordial power spectrum from Figure 2 translate into the angular power spectrum of the temperature CMB fluctuations, shown as $\ell^3(\ell+1)C_\ell^{TT}/2\pi$ mK² (left panel) to highlight the higher order peaks. The dashed vertical lines show the multipoles corresponding to the wavenumbers under consideration, using $\ell = kd$; these wavenumbers as shown for the high- k bands. The dark (light) band shows the 1σ region for the C_ℓ^{TT} spectra for the ACT+WMAP (WMAP only) data. The best-fit curve using the combination of ACT and WMAP data is shown as the dark solid curve and the dashed black curve shows the best-fit power-law spectrum from Dunkley et al. (2010). The right panel shows the corresponding C_ℓ^{TE} power spectrum, plotted here as $\ell(\ell+1)C_\ell^{TE}/2\pi$ μ K², together with WMAP data and data from the QUaD experiment (Brown et al. 2009).

TABLE 2
ESTIMATED MODEL PARAMETERS AND 68% CONFIDENCE LIMITS FOR THE ACT 2008
SOUTHERN SURVEY DATA COMBINED WITH WMAP

	Parameter ^a	ACT+WMAP Power-law ^b	ACT + WMAP binned $P(k)$ with H_0 prior
Primary	$100\Omega_b h^2$	2.222 ± 0.055	2.307 ± 0.124
	$\Omega_c h^2$	0.1125 ± 0.0053	0.1166 ± 0.0085
	θ_A	1.0394 ± 0.0024	1.0419 ± 0.0034
	τ	0.086 ± 0.014	0.100 ± 0.017
Secondary	A_p	15.81 ± 2.01	14.19 ± 2.45
	A_c	< 10.44	< 17.08
	A_{SZ}	< 0.92	< 1.55

^a For one-tailed distributions, the upper 95% confidence limit is given, whereas the 68% limits are shown for two-tailed distributions.

^b The power-law model for the primordial spectrum is $\mathcal{P}(k) = \Delta_{\mathcal{R}}^2 \left(\frac{k}{k_0}\right)^{n_s-1}$

ther varies significantly as the cosmological parameters are varied within their errors in the flat cosmology we consider in this work. The $P(k)$ constraints from the CMB alone overlap well with the power spectrum measurements from the SDSS DR7 LRG sample (Reid et al. 2010), which have been deconvolved from their window functions. The ACT data allow us to probe the power spectrum today at scales $0.001 < k < 0.19$ Mpc⁻¹ using only the CMB, improving on previous constraints using microwave data. In addition, the lensing deflection power spectrum also provides a constraint on the amplitude of matter fluctuations at a comoving wavenumber of $k \simeq 0.015$ Mpc⁻¹ at a redshift $z \simeq 2$. The recent measurement of CMB lensing by ACT (Das et al. 2011) is shown as $P(k = 0.015 \text{ Mpc}^{-1}) = 1.16 \pm 0.29 \text{ Mpc}^3$ on Figure 5. These two measurements are consistent with each other and come from two independent approaches:

the lensing deflection power is a direct probe of the matter content at this scale (with only a minor projection from $z = 2$ to $z = 0$), while the primordial power is projected from the scales at the surface of last scattering at $z \simeq 1040$ to the power spectrum today.

Finally, cluster measurements provide an additional measurement of the matter power spectrum on a characteristic scale k_c , corresponding to the mass of the cluster, $M_c = (4\pi/3)\rho_m(\pi/k_c)^3$, where ρ_m is the matter density of the universe today. We compute the amplitude of the power spectrum at the scale k_c from reported σ_8 values as

$$P_c(k_c, z = 0) = (\sigma_8/\sigma_{8,\Lambda\text{CDM}})P(k_c, z = 0)_{\Lambda\text{CDM}}, \quad (5)$$

where $\sigma_{8,\Lambda\text{CDM}} = 0.809$ is the concordance ΛCDM value (Larson et al. 2010). We use the measurement of $\sigma_8 = 0.851 \pm 0.115$ from clusters detected by ACT, at a charac-

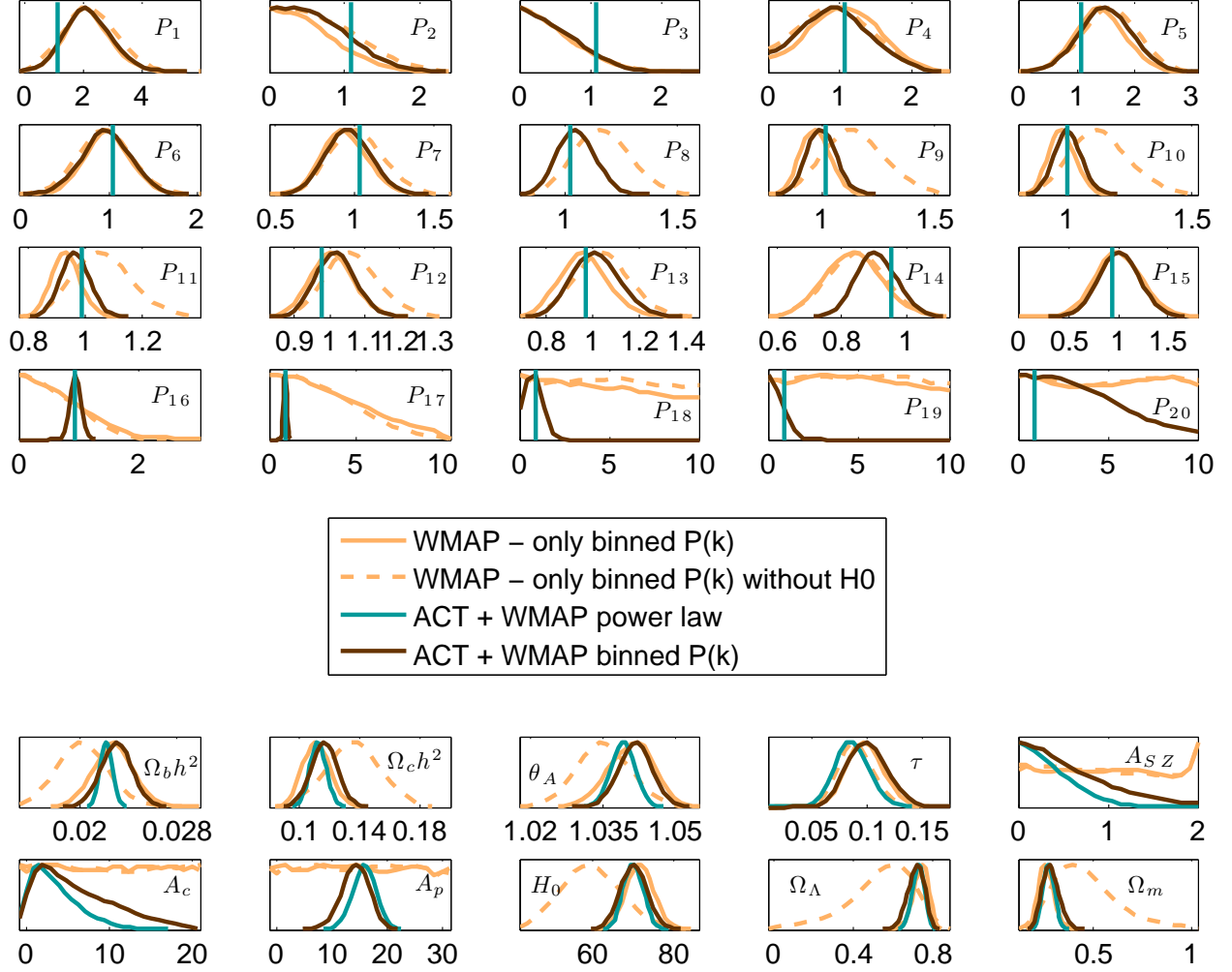


FIG. 4.— Parameter constraints: marginalized one dimensional distributions for the parameters determined from the ACT and WMAP data. The top 20 panels in the figure show the likelihoods for the power spectrum parameters determined using MCMC methods, while the lower 10 panels show the primary and secondary cosmological parameters and 3 derived quantities: the Hubble parameter H_0 , the dark energy density Ω_Λ , and the matter density Ω_m . The light solid curves show the constraints on the parameters from ACT in combination with WMAP data for the Λ CDM case — the vertical lines in the power spectrum panels show the values the power spectrum would take assuming the best-fit $n_s = 0.963$ power-law from Dunkley et al. (2010). The parameter constraints for this power-law Λ CDM model is shown as the light curves. The solid dark lines show the distributions from ACT and WMAP data, assuming a prior on the Hubble constant. The best-fit value of the power-law spectral index obtained from fitting the well-constrained bands ($P_5 - P_{17}$) is $n_s = 0.965$. The dashed curves indicate the degeneracy between low values of θ_A and primordial power in modes around the position of the first peak.

teristic mass of $M = 10^{15} M_\odot$ (Sehgal et al. 2011), as well as measurements from the Chandra Cosmology Cluster Project (CCCP) (Vikhlinin et al. 2009), measured from the 400 square degree ROSAT cluster survey (Burenin et al. 2007). The quoted value of $\sigma_8 = 0.813 \pm 0.013$ is given at a characteristic mass of $2.5 \times 10^{14} h^{-1} M_\odot$. In addition, we illustrate constraints from galaxy clustering calibrated with weak lensing mass estimates of brightest cluster galaxies (BCG) (Tinker et al. 2011), quoted as $\sigma_8 = 0.826 \pm 0.02$. In this case, we compute the characteristic mass M_c (and hence k_c) from the inverse variance weighted average mass of the halos (from Table 2 in Tinker et al. (2011)) as $M_c = 4.7 \times 10^{13} h^{-1} M_\odot$. To remove the dependence on cosmology, the CCCP and BCG mass

measurements are multiplied by a factor of h^{-1} (where $h = 0.738$ is taken from the recent Riess et al. (2011) result). The ACT cluster measurement, however, is already expressed in solar mass units, and hence this operation is not required.

Power spectrum constraints from measurements of the Lyman- α forest are shown at the smallest scales probed. The slanted errorbars for the SDSS and Lyman- α data reflect the uncertainty in the power spectrum measurement from the Hubble constant uncertainty alone. Again, these data are normally plotted as a function of $h^{-1} \text{Mpc}$, hence we propagate the 1σ error on the Hubble parameter from Riess et al. (2011) through to the plotted

error region in both wavenumber and power spectrum.

Transforming from units of power spectrum to mass variance $\Delta_M/M = \sqrt{P(k)k^3/(2\pi^2)}$ (indicated in the bottom panel of Figure 5), allows one to visualize directly the relationship between mass scale and variance. While $\Delta_M/M \simeq 1$ for $10^{16} M_\odot$ galaxies, the variance decreases as the mass increases and we probe the largest scales, covering ten orders of magnitude in the range of masses of the corresponding probes.

4. CONCLUSIONS

We constrained the primordial power spectrum as a function of scale in 20 bands using a combination of data from the 2008 Southern Survey of the Atacama Cosmology Telescope and WMAP data. We make no assumptions about the smoothness of the power spectrum, beyond a spline interpolation between power spectrum bands. The arcminute resolution of ACT constrains the power spectrum at scales $0.1 < k < 0.19 \text{ Mpc}^{-1}$ which had not yet been well constrained by microwave background experiments. This allows us to test for deviations from scale invariance in a model-independent framework. We find no significant evidence for deviation from a power-law slope. When a power-law spectrum is fit to our well-constrained bands, our best-fit slope of $n_s = 0.965$ is consistent with that determined directly from a standard parameter space of Λ CDM models with a power-law spectrum, using the same data. Mapping the primordial power to the late-time power spectrum using the fluctuations in the matter density, we obtain measurements of the power spectrum today from the cosmic microwave background which are consistent with results from galaxy redshift surveys, but which also probe the power spectrum to

much larger scales, $k \simeq 0.001 \text{ Mpc}^{-1}$, over mass ranges $10^{15} - 10^{22} M_\odot$. Finally, the allowed range in the primordial power from the high- ℓ ACT temperature power spectrum measurements constrains the allowed range in the polarization-temperature cross spectrum, which will be probed with future polarization experiments.

This work was supported by the U.S. National Science Foundation through awards AST-0408698 for the ACT project, and PHY-0355328, AST-0707731 and PIRE-0507768. Funding was also provided by Princeton University and the University of Pennsylvania, Rhodes Trust (RH), RCUK Fellowship (JD), ERC grant 259505 (JD), NASA grant NNX08AH30G (SD, AH and TM), NSERC PGSD scholarship (ADH), NSF AST-0546035 and AST-060697 (AK), NSF Physics Frontier Center grant PHY-0114422 (ES), SLAC no. DE-AC3-76SF0051 (NS), and the Berkeley Center for Cosmological Physics (SD) Computations were performed on the GPC supercomputer at the SciNet HPC Consortium. We thank Reed Plimpton, David Jacobson, Ye Zhou, Mike Cozza, Ryan Fisher, Paula Aguirre, Omelan Stryzak and the Astro-Norte group for assistance with the ACT observations. We also thank Jacques Lassalle and the ALMA team for assistance with observations. RH thanks Seshadri Nadathur for providing the best-fit power spectrum void models and Chris Gordon, David Marsh and Joe Zuntz for useful discussions. ACT operates in the Chajnantor Science Preserve in northern Chile under the auspices of the Commission Nacional de Investigacin Cientifica y Tecnolgica (CONICYT). Data acquisition electronics were developed with assistance from the Canada Foundation for Innovation.

REFERENCES

- Achúcarro, A., Gong, J., Hardeman, S., Palma, G. A., & Patil, S. P. 2011, JCAP, 1, 30, 1010.3693
- Adams, J., Cresswell, B., & Easter, R. 2001, Phys. Rev. D, 64, 123514, arXiv:astro-ph/0102236
- Amendola, L., Gottloeber, S., Muckett, J. P., & Mueller, V. 1995, ApJ, 451, 444, arXiv:astro-ph/9408104
- Atrio-Barandela, F., Einasto, J., Gottlöber, S., Müller, V., & Starobinsky, A. 1997, Soviet Journal of Experimental and Theoretical Physics Letters, 66, 397, arXiv:astro-ph/9708128
- Barnaby, N., & Huang, Z. 2009, Phys. Rev. D, 80, 126018, 0909.0751
- Bird, S., Peiris, H. V., Viel, M., & Verde, L. 2010, ArXiv e-prints, 1010.1519
- Blanchard, A., Douspis, M., Rowan-Robinson, M., & Sarkar, S. 2003, Astron. Astrophys., 412, 35, astro-ph/0304237
- Bridges, M., Feroz, F., Hobson, M. P., & Lasenby, A. N. 2009, MNRAS, 400, 1075, ADS, 0812.3541
- Bridges, M., Lasenby, A. N., & Hobson, M. P. 2007, MNRAS, 381, 68, ADS, arXiv:astro-ph/0607404
- Bridle, S. L., Lewis, A. M., Weller, J., & Efstathiou, G. 2003, MNRAS, 342, L72, ADS
- Brown, M. L. et al. 2009, ApJ, 705, 978, ADS, 0906.1003
- Burenin, R. A., Vikhlinin, A., Hornstrup, A., Ebeling, H., Quintana, H., & Mescheryakov, A. 2007, ApJS, 172, 561, ADS, arXiv:astro-ph/0610739
- Carlstrom, J. E. et al. 2009, ArXiv e-prints, ADS, 0907.4445
- Chantavat, T., Gordon, C., & Silk, J. 2010, ArXiv e-prints, 1009.5858
- Das, S. et al. 2010, arXiv:1009.0847, ADS, 1009.0847
- , 2011, ArXiv e-prints, 1103.2124
- Dunkley, J., Bucher, M., Ferreira, P. G., Moodley, K., & Skordis, C. 2005, MNRAS, 356, 925, ADS, arXiv:astro-ph/0405462
- Dunkley, J. et al. 2010, arXiv:1009.0866, ADS, 1009.0866
- Easter, R., & Peiris, H. 2006, JCAP, 0609, 010, astro-ph/0604214
- Einasto, J., Einasto, M., Tago, E., Starobinsky, A. A., Atrio-Barandela, F., Müller, V., Knebe, A., & Cen, R. 1999, ApJ, 519, 469, arXiv:astro-ph/9812249
- Fowler, J. W. et al. 2010, ApJ, 722, 1148, ADS, 1001.2934
- Hajian, A. et al. 2010, arXiv:1009.0777, ADS, 1009.0777
- Hannestad, S. 2003, JCAP, 0305, 004, astro-ph/0303076
- Hincks, A. D. et al. 2009, arXiv:0907.0461, ADS, 0907.0461
- Hunt, P., & Sarkar, S. 2007, Phys. Rev. D, 76, 123504, 0706.2443
- Kates, R., Muller, V., Gottloeber, S., Muckett, J. P., & Retzlaff, J. 1995, MNRAS, 277, 1254, arXiv:astro-ph/9507036
- Kinney, W. H. 2001, Phys. Rev. D, 63, 043001, arXiv:astro-ph/0005410
- Kinney, W. H., Kolb, E. W., Melchiorri, A., & Riotto, A. 2006, Phys. Rev., D74, 023502, astro-ph/0605338
- Komatsu, E. et al. 2010, arXiv:1001.4538, ADS, 1001.4538
- Komatsu, E., & Spergel, D. N. 2001, Phys. Rev. D, 63, 063002, ADS, arXiv:astro-ph/0005036
- Kosowsky, A., & Turner, M. S. 1995, Phys. Rev. D, 52, 1739
- Larson, D. et al. 2010, arXiv:1001.4635, ADS, 1001.4635
- Lasenby, A., & Doran, C. 2003, astro-ph/0307311
- Lewis, A., & Bridle, S. 2002, Phys. Rev. D, 66, 103511, arXiv:astro-ph/0205436
- Lewis, A., & Challinor, A. 2002, Phys. Rev. D, 66, 023531, arXiv:astro-ph/0203507
- Liddle, A. R. 2004, Monthly Notices of the Royal Astronomical Society, 351, L49
- Lueker, M. et al. 2010, ApJ, 719, 1045, ADS, 0912.4317
- Marriage, T. A. et al. 2010, ArXiv e-prints, ADS, 1010.1065
- Matsumiya, M., Sasaki, M., & Yokoyama, J. 2002, Phys. Rev. D, 65, 083007, arXiv:astro-ph/0111549
- McDonald, P. et al. 2006, ApJS, 163, 80, ADS, arXiv:astro-ph/0405013

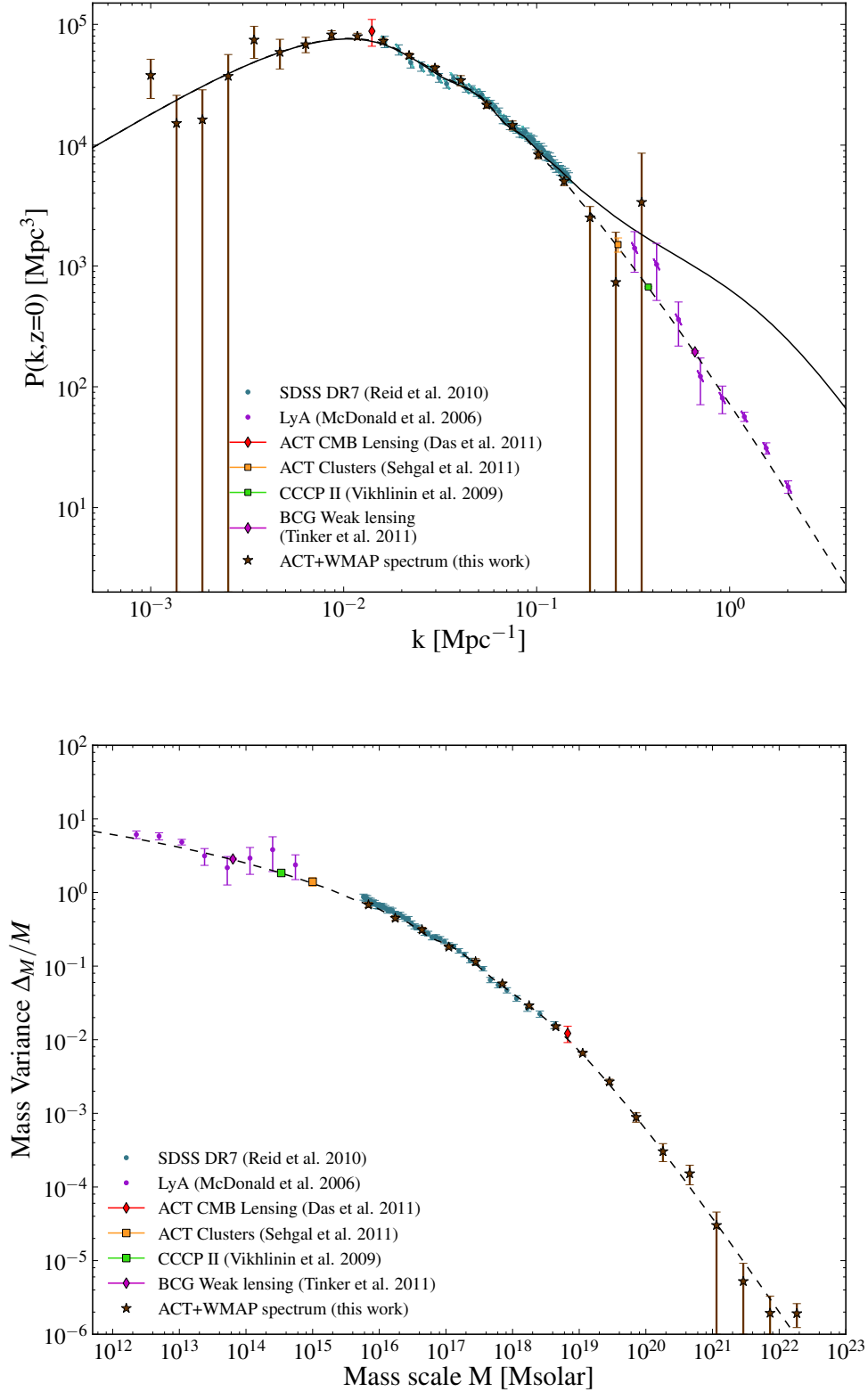


FIG. 5.— The reconstructed matter power spectrum: the stars show the power spectrum from combining ACT and WMAP data (top panel). The solid and dashed lines show the nonlinear and linear power spectra respectively from the best-fit ACT Λ CDM model with spectral index of $n_s = 0.96$ computed using CAMB and HALOFIT (Smith et al. 2003). The data points between $0.02 < k < 0.19 \text{ Mpc}^{-1}$ show the SDSS DR7 LRG sample, and have been deconvolved from their window functions, with a bias factor of 1.18 applied to the data. This has been rescaled from the Reid et al. (2010) value of 1.3, as we are explicitly using the Hubble constant measurement from Riess et al. (2011) to make a change of units from $h^{-1}\text{Mpc}$ to Mpc . The constraints from CMB lensing (Das et al. 2011), from cluster measurements from ACT (Sehgal et al. 2011), CCCP (Vikhlinin et al. 2009) and BCG halos (Tinker et al. 2011), and the power spectrum constraints from measurements of the Lyman- α forest (McDonald et al. 2006) are indicated. The CCCP and BCG masses are converted to solar mass units by multiplying them by the best-fit value of the Hubble constant, $h = 0.738$ from Riess et al. (2011). The bottom panel shows the same data plotted on axes where we relate the power spectrum to a mass variance, Δ_M/M , and illustrates how the range in wavenumber k (measured in Mpc^{-1}) corresponds to range in mass scale of over 10 orders of magnitude. Note that large masses correspond to large scales and hence small values of k . This highlights the consistency of power spectrum measurements by an array of cosmological probes over a large range of scales.

- Menanteau, F. et al. 2010, ApJ, 723, 1523, ADS, 1006.5126
- Mukherjee, P., & Wang, Y. 2003, ApJ, 599, 1, ADS
- Nadathur, S., & Sarkar, S. 2010, ArXiv e-prints, 1012.3460
- Niemack, M. D. et al. 2010, in Society of Photo-Optical Instrumentation Engineers (SPIE) Conference Series, Vol. 7741, Society of Photo-Optical Instrumentation Engineers (SPIE) Conference Series, 1006.5049, ADS
- Peiris, H. V., & Verde, L. 2010, Phys. Rev. D, 81, 021302, 0912.0268
- Planck Collaboration et al. 2011, ArXiv e-prints, ADS, 1101.2022
- Press, W. H., Teukolsky, S. A., Vetterling, W. T., & Flannery, B. P. 1992, Numerical Recipes in C: The Art of Scientific Computing, 2nd edn. (Cambridge University Press)
- Reichardt, C. L. et al. 2009, ApJ, 694, 1200, ADS, 0801.1491
- Reid, B. A. et al. 2010, MNRAS, 404, 60, ADS, 0907.1659
- Riess, A. G. et al. 2011, ApJ, 730, 119, ADS, 1103.2976
- . 2009, ApJ, 699, 539, ADS, 0905.0695
- Sealfon, C., Verde, L., & Jimenez, R. 2005, Phys. Rev. D, 72, 103520, ADS, arXiv:astro-ph/0506707
- Sehgal, N. et al. 2011, ApJ, 732, 44, 1010.1025
- Shafieloo, A., & Souradeep, T. 2007, ArXiv e-prints, 709, ADS, 0709.1944
- Sherwin, B. D. et al. 2011, ArXiv e-prints, ADS, 1105.0419
- Sievers, J. L. et al. 2009, arXiv:0901.4540, ADS, 0901.4540
- Silk, J. 1968, ApJ, 151, 459
- Smith, R. E. et al. 2003, MNRAS, 341, 1311, ADS, arXiv:astro-ph/0207664
- Spergel, D. N. et al. 2007, ApJS, 170, 377, arXiv:astro-ph/0603449
- Swetz, D. S. et al. 2010, arXiv:1007.0290, ADS, 1007.0290
- Takeuchi, T. 2000, Astrophysics and Space Science, 271, 213
- Tegmark, M., & Zaldarriaga, M. 2002, Phys. Rev. D, 66, 103508, arXiv:astro-ph/0207047
- Tinker, J. L. et al. 2011, ArXiv e-prints, ADS, 1104.1635
- Vazquez, J. A., Lasenby, A. N., Bridges, M., & Hobson, M. P. 2011, ArXiv e-prints, ADS, 1103.4619
- Verde, L., & Peiris, H. 2008, JCAP, 7, 9, ADS, 0802.1219
- Vikhlinin, A. et al. 2009, ApJ, 692, 1060, ADS, 0812.2720
- Wang, Y., Spergel, D. N., & Strauss, M. A. 1999, ApJ, 510, 20, ADS, arXiv:astro-ph/9802231